

## HIGH-EFFICIENT PAIR MAGNETIC SPECTROMETER

P. I. GOLUBNICHYI, L. M. KURDADZE, D. M. NIKOLENKO, A. P. ONUCHIN, S. G. POPOV and V. A. SIDOROV

*Institute of Nuclear Physics of the Siberia Department of the Academy of Sciences of the USSR, Novosibirsk, USSR*

Received 27 June 1968

A magnetic pair spectrometer for  $\gamma$  rays using a spark chamber is described. The spectrometer has been calibrated with a monochromatic beam of 120-MeV  $\gamma$  rays. For a target thickness of  $0.014 X_0$  the resolution is 1.5%. We have studied the possibility of using the spectrometer with a thick target (up to  $0.3 X_0$ )

### 1. Introduction

Of the known methods of measuring  $\gamma$ -ray energy in the region of tens and hundreds of MeV, the best energy resolution is provided by a magnetic pair spectrometer. Such spectrometers have been used in many laboratories<sup>1-7</sup>). The method consists of measuring, by means of a magnetic field, the combined energy of an electron-positron pair produced in a thin target.

In earlier studies, two counters connected in coincidence were used to detect the pair<sup>1</sup>). Increasing the accuracy of the measurements in such devices results in a sharp drop in detection efficiency. To avoid this difficulty, multichannel systems, consisting of a large number of counters came into use<sup>3-5,7</sup>). Besides the efficiency increase, the advantage of multichannel spectrometers is the possibility of simultaneous measurement of  $\gamma$ -rays of different energies. The resolution achieved in the multichannel spectrometer is 5-15% (fwhm).

In such systems, the improvement of the energy resolution, without reduction of the efficiency, requires a sharp increase in the number of counters and coincidence circuits.

The development of spark chamber techniques has provided the possibility of improving spectrometer energy resolution. Recently, Leslie and Main<sup>8</sup>) have described the use of spark chambers in a pair spectrometer. They obtained a resolution of 3%.

The efficiency of a pair spectrometer is determined by the probability  $W_t$  of pair production in the target and the probability  $W_d$  for detection of the pair. The probability  $W_d$  is determined by the design of the system which detects the electrons and positrons. For practical reasons the counters in multichannel spectrometers do not intercept all particle trajectories and  $W_d$  is at best only about 0.3. A spark chamber does not have dead zones and in principle permits making  $W_d$  close to 1.

Further increase of spectrometer efficiency is possible

without appreciable loss of resolution. For this purpose the ionization and bremsstrahlung losses of the pair were measured with NaI(Tl) counters. For an effective target, of thickness  $0.1 X_0$ , the resolution is 2.3% and the efficiency 6%.

only by increasing the target thickness. As a rule, target thicknesses of the order of 0.01 radiation length  $X_0$  are used in experiments. The probability of pair production by a  $\gamma$  ray of 100 MeV is about 1% for such a target. The use of a thicker target leads to a loss of accuracy in the measurement of the  $\gamma$ -ray energy, since ionization and bremsstrahlung losses and multiple scattering in the target begin to play an appreciable role.

In the present work we have investigated the possibility of using a thick target (up to  $0.3 X_0$ ) in a pair spectrometer without appreciable loss of energy resolution. For this purpose we have used as target a NaI(Tl) crystal, in which the energy loss by ionization is measured. We have used a NaI(Tl) total absorption counter to measure the energy loss by radiation.

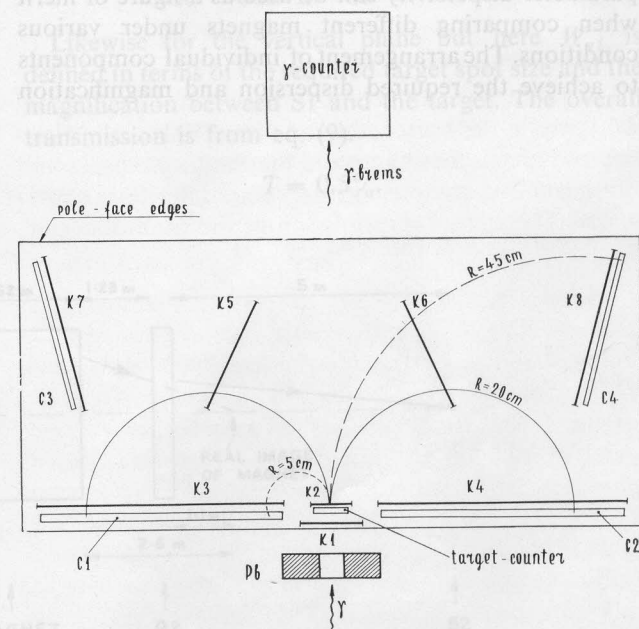


Fig. 1. Geometrical arrangement of the spectrometer: K - spark chambers; C - scintillation counters.

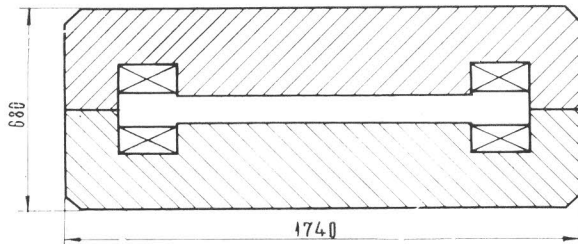


Fig. 2. Magnet cross section in a vertical plane, perpendicular to the  $\gamma$ -ray beam.

To reduce the effect of multiple scattering on the accuracy of the energy measurement, the radius of curvature for electrons and positrons of high-energy is determined from three points. Detection of electrons and positrons is accomplished by wire spark chambers with ferrite-core memories.

## 2. Spectrometer design

Fig. 1 shows the geometrical arrangement of the spectrometer. The point of formation of the pair is defined by chamber K2. Chamber K1 is placed in front of the target. Up to a radius of curvature of about 25 cm, the electron energy is determined in the usual way with  $180^\circ$  focusing, from two points (chambers K3 and K4). For larger radii the energy is determined from three points (K2, K6, K8 or K2, K5, K7). The use of three chambers eliminates errors associated with the angle of emission of the particle from the target. In addition, use of  $180^\circ$  focusing up to the maximum energy of the particles would lead to an increase in size and power of the magnet by a factor of two.

Triggering of the spark chambers is initiated by any double coincidence between counter groups (C1, C3) and (C2, C4). The scintillators are of polystyrene plastic, 1 cm thick. The light is carried outside the magnet by plexiglas light pipes about 40 cm long. The counters use FEU-30 photomultipliers.

The target-counter is a NaI(Tl) crystal  $50 \times 70 \text{ mm}^2$  in area and 9 mm thick. Bremsstrahlung  $\gamma$ -rays are detected by a total-absorption counter ( $\gamma$ -counter) consisting of an NaI(Tl) crystal 190 mm in dia. and 160 mm thick. The light is collected by a FEU-65 photomultiplier.

The construction of the magnet is shown in fig. 2. The magnet yoke is closed on all sides. This arrangement of the yoke provides good shielding of the photomultipliers from the magnetic field. The magnet gap is 10 cm. The spark chambers are located at least 5 cm from the edge of the magnet poles. The error in the determination of the particle energy associated with the inhomogeneity of the magnetic fields, does not exceed 0.2%. The magnet current is supplied by a dc generator with electronic stabilization. The stability of the magnet is monitored by nuclear magnetic resonance.

The spark chambers consist of fiberglass-base textolite frames 10 mm thick, on both sides of which are stretched 0.1 mm copper wires with a spacing of 1 mm. The wires on one side are soldered together and are used as the high-voltage electrode. The wires of the ground electrode are soldered individually to a plait of wires which is led outside the magnet to a matrix of ferrite cores (the length of the plait is about 3 m). The working height of the chambers is 70 mm.

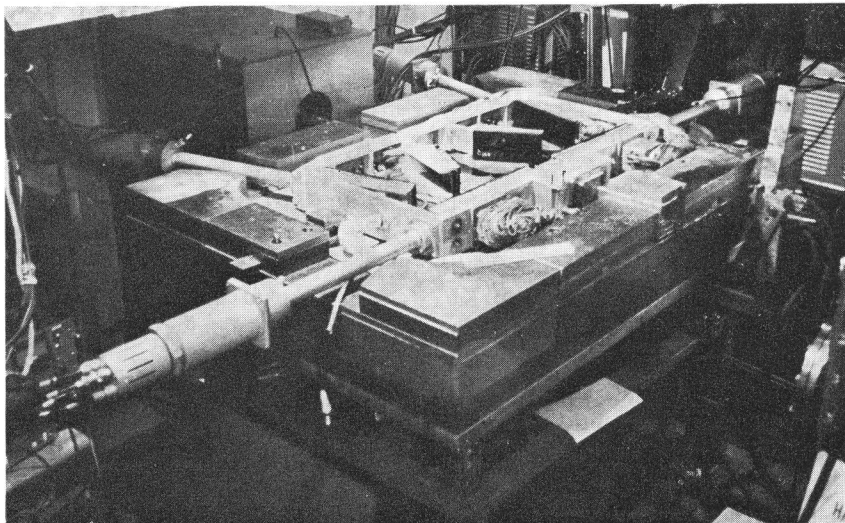


Fig. 3. View of spectrometer with upper half of magnet removed.

The general appearance of the spectrometer is shown in fig. 3. The spark chamber and scintillators are included in the vacuum chamber; the top and bottom of the vacuum chamber are formed by the magnet poles, and the walls are made of duraluminum sealed with rubber gaskets. The  $\gamma$ -ray beam enters and leaves the vacuum through flanges covered with 0.1 mm stainless steel.

During the testing of the spark chambers it was observed that a strong optical coupling existed between the chambers. A spark in one chamber resulted in discharges in the other chambers, even if particles had not passed through them. To avoid this effect, it was necessary to cement over each chamber a mylar film coated with epoxy-resin containing lampblack. The thickness of this film was  $0.015 \text{ g/cm}^2$ .

The entire vacuum chamber was pumped to a fore vacuum and filled with the working gas (helium +3% alcohol) to a pressure of 1.1 atm. The helium filling is advantageous in this case with respect to the scattering of particles in the space between the chambers. The gas was replaced every three days.

The spark chambers operated with a pulse height of 9 kV. Under these conditions spurious sparks are completely absent, and the efficiency of the chambers is 96–99%. During the experiment the chamber efficiency is monitored by means of chambers K2, K5 and K6.

Information from the spark chambers is recorded on a perforated tape. On this same tape are punched the pulse heights from the target-counter and  $\gamma$ -counter. The results are analysed with a Minsk-22 computer.

### 3. Calculation of resolution and efficiency for a thin target

We will denote as "thin" any target in which the ionization and bremsstrahlung losses can be neglected. A target of thickness  $0.014 X_0$  ( $50 \mu\text{m}$  of tungsten) was chosen for our experiment.

The energy resolution of the spectrometer is determined mainly by the following effects: the spatial resolution of the chambers; multiple scattering in the helium, in the lightproofing of chambers K5 and K6, and in the target. The calculated accuracies of the measurement of the electron energy are given in table 1, for a magnetic field strength of 9 kG. Results are given for several radii of curvature. The resolution  $\delta$  always refers to the relative full width at half height.

The rms error  $\sigma$  in the determination of the point of passage of a particle through a spark chamber is taken equal to  $\frac{1}{3} \Delta$ , in accordance with Fischer's review<sup>9)</sup>,

where  $\Delta$  is the spacing between wires. The distribution function is assumed to be Gaussian.

TABLE I

Contribution of various effects to the error in electron energy measurement  $\delta$  (%).

Effect	Electron radius of curvature (cm)				
	5	10	20	30	40
Spatial resolution of chamber	1.1	0.6	0.3	0.45	0.5
Scattering in helium	0.7	0.5	0.4	0.3	0.2
Scattering in light-proofing of chambers K5, K6	—	—	—	1.1	0.8
Scattering in target ( $t = 0.014 X_0$ )	1.3	0.3	—	—	—
Combined effect	1.8	0.9	0.5	1.2	1

The accuracy of the measurement of the combined energy of the pair depends on the relation of the radii of curvature of the two particles. For the  $\gamma$ -ray energy of interest here, 120 MeV, the average value of resolution is 1%.

It should be noted that in table 1 we have not taken into account the scattering of particles by the wires of spark chambers K5 and K6. Since the transparency of the chambers is 80%, 20% of the particles passing through a chamber will hit a wire. The rms scattering angle in the wires is three times that in the lightproofing film. The effect should produce tails in the distribution. The probability  $W_d$  for detection of a pair depends on the minimum and maximum radii of curvature of particle trajectories which can enter the chambers.

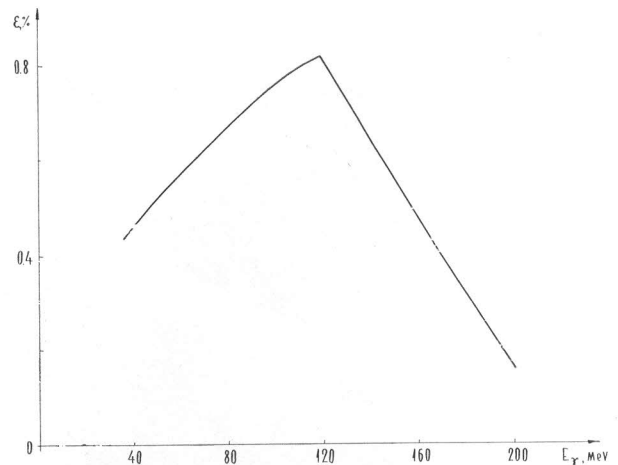


Fig. 4. Spectrometer efficiency as a function of  $\gamma$ -ray energy. Target thickness  $0.014 X_0$ , magnetic field 9 kG.

In our case these radii are respectively 3.5 and 45 cm. For a magnetic field strength  $H = 9$  kG and a  $\gamma$ -ray energy of 120 MeV,  $W_d = 0.88$ , and the  $\gamma$ -ray detection efficiency for a target thickness  $0.014 X_0$  is  $\varepsilon = 0.81\%$ . The detection efficiency for  $\gamma$ -rays of other energies is shown in fig. 4.

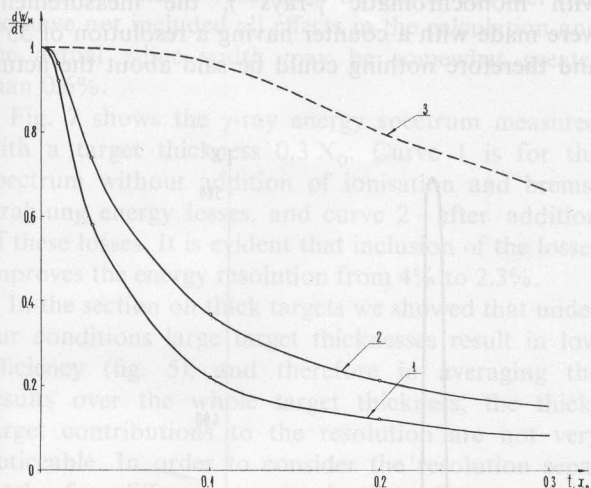


Fig. 5. Pair detection probability associated with multiple scattering in the target, as a function of the depth at which the pair is produced, for a total radius of curvature of 45 cm: 1. Equal radii of curvature; 2. Radius of one particle 5 cm and of the other 40 cm; 3. Similar to curve 1, but calculated for  $H = 15$  kG and a chamber height of 15 cm.

#### 4. Calculation of resolution and efficiency for a thick target

In calculating the detection probability of a pair for a thick target, it is necessary to take into account multiple scattering of electrons and positrons in the target. The detection probability  $W_d$  can be conveniently written in the form  $W_d = W_R \cdot W_M$ , where  $W_R$  is the detection probability associated with emission of a pair of particles outside the allowed limits of the radius of curvature, and  $W_M$  is the detection probability associated with excursion of a particle beyond the vertical limits of the chambers as the result of multiple scattering. Since the multiple scattering angles depend on the depth of creation of the pair in the target, it is convenient to express this effect as a function of the remaining target thickness  $t$ , which the particles traverse. Fig. 5 shows the probability  $W_M$  as a function of depth in the target for a total radius of curvature of the pair of 45 cm ( $\gamma$ -ray energy 120 MeV). Curve 1 is for equal radii of the two particles (the case corresponds to  $180^\circ$  focusing for both particles), and curve 2 is for radii of 5 and 40 cm. All other cases lie between these curves.

The pair detection probability  $W_M$  for large target thicknesses depends roughly quadratically on the magnetic field and chamber height. Curve 3 in fig. 5 is similar to curve 1 but is calculated for a field of 15 kG and a chamber height of 15 cm.

For our conditions and a target thickness of  $0.3 X_0$  the average pair detection probability associated with multiple scattering is  $W_M = 0.3$ . Thus, the effective thickness is  $0.1 X_0$ . The detection efficiency for a 120-MeV  $\gamma$ -ray is  $\varepsilon = 6\%$ . In the calculation of the resolution of the spectrometer, in addition to the effects discussed in the section on thin targets, it is necessary to take into account the accuracy with which the ionisation and bremsstrahlung losses are measured, and also to consider again the effect of multiple scattering in the target.

Multiple scattering in the target is important only in the region of  $180^\circ$  focusing. Averaging of the resolution over different combinations of the pair energy shows that the average accuracy of measurement of a combined electron and positron energy of 120 MeV is 1.5%.

The error in measurement of the ionisation loss is associated with the fluctuations of the pulse height from the photomultipliers. The counter resolution for  $^{137}\text{Cs}$  (0.66 MeV) is 30%. This means that for a 120-MeV  $\gamma$ -ray the error due to measurement of the ionisation loss for a pair produced at a depth  $0.3 X_0$  should not exceed 0.7%. The corresponding error for a depth of  $0.1 X_0$  is 0.4%.

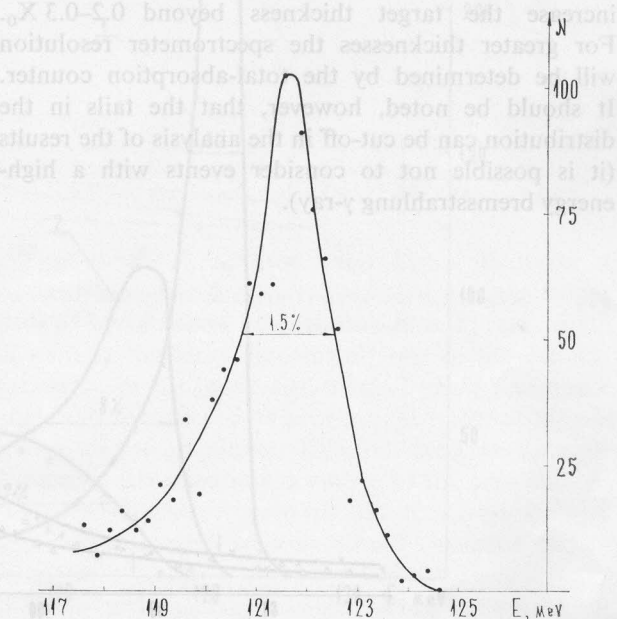


Fig. 6. Gamma-ray energy spectrum measured with a target thickness  $0.014 X_0$ .



For the errors associated with the measurement of the energy of the bremsstrahlung  $\gamma$  rays we can make only crude estimates, principally because the counter resolution is not known over the entire  $\gamma$ -ray energy region of interest to us. In the  $\gamma$ -ray energy region (40–120 MeV), the counter resolution measured in the same apparatus<sup>10</sup>, is about 35%. In the 1-MeV region the resolution is about 30%. No data are available in the region 1–40 MeV. We can assume that in the low energy region up to about 15 MeV, the probability of shower formation is small and the resolution varies as  $E^{-\frac{1}{2}}$ . It is difficult to say anything definite about the region of transition to showers.

The probability of radiation by an electron in passing through  $t$  radiation lengths of matter can be found from the Bethe-Heitler formula

$$dW = (dE/E_0) \{ \ln(E_0/E)^{(t/\ln 2)-1} / \Gamma(t/\ln 2) \},$$

where  $E_0$  and  $E$  are the initial and final energies of the electron. This function has a long tail in the region of high radiation energies, and the probability of radiating energy increases substantially with increasing thickness  $t$ .

Let us consider for example  $t = 0.25 X_0$ . In 30% of the cases the electron radiates an energy greater than 0.3 of its initial energy, and in 40% of the cases it will be greater than 0.2. If we take the error in the counter measurement to be 35%, this means that for a 120-MeV  $\gamma$ -ray an error of more than 7% will be made in 30% of the cases, and of more than 4% in 40% of the cases.

These estimates show that it is unreasonable to increase the target thickness beyond 0.2–0.3  $X_0$ . For greater thicknesses the spectrometer resolution will be determined by the total-absorption counter. It should be noted, however, that the tails in the distribution can be cut-off in the analysis of the results (it is possible not to consider events with a high-energy bremsstrahlung  $\gamma$ -ray).

## 5. Results of the calibration

Calibration of the spectrometer was performed in the monochromatic  $\gamma$ -ray beam from the electron storage ring<sup>10</sup> VEP-1. The measurements were made at a  $\gamma$ -ray energy of 120 MeV. The calculated value of the  $\gamma$ -ray line width is about 0.6%. In our first work with monochromatic  $\gamma$ -rays<sup>10</sup>, the measurements were made with a counter having a resolution of 35% and therefore nothing could be said about the actual

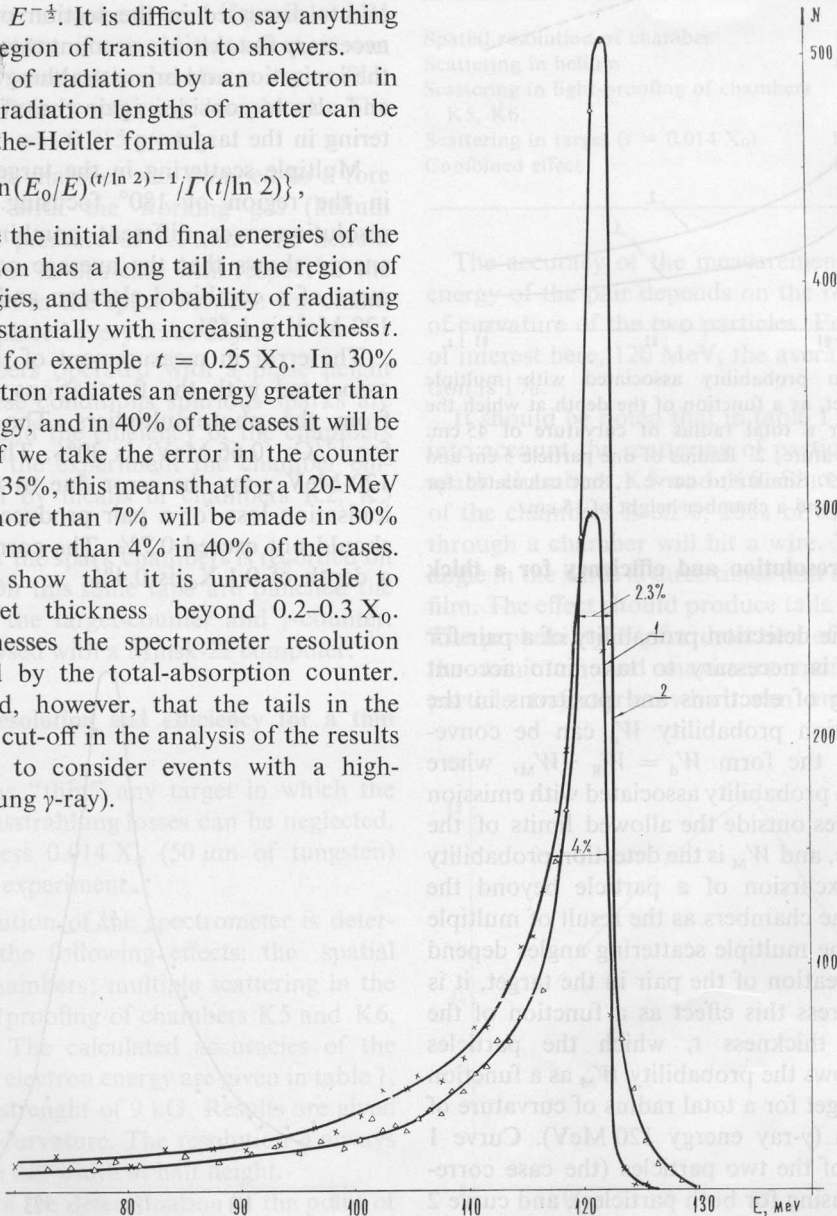


Fig. 7. Gamma-ray energy spectrum measured with a target thickness  $0.3 X_0$ , without (1) and with (2) correction for ionisation and bremsstrahlung losses.

line width. In this sense the present work is not only a test of the spectrometer but also of the first measurements of the  $\gamma$ -ray line width.

Fig. 6 shows the  $\gamma$ -ray energy spectrum measured with a 50- $\mu$ m tungsten target. The width at half height is 1.5%. Some excess of the experimental resolution over the calculated value may be due to the fact that we have not included all effects in the calculation and the actual  $\gamma$ -line width may be somewhat greater than 0.6%.

Fig. 7 shows the  $\gamma$ -ray energy spectrum measured with a target thickness  $0.3 X_0$ . Curve 1 is for the spectrum without addition of ionisation and bremsstrahlung energy losses, and curve 2 - after addition of these losses. It is evident that inclusion of the losses improves the energy resolution from 4% to 2.3%.

In the section on thick targets we showed that under our conditions large target thicknesses result in low efficiency (fig. 5), and therefore in averaging the results over the whole target thickness, the thick-target contributions to the resolution are not very noticeable. In order to consider the resolution separately for different target depths, all events were divided into three groups according to the depth of pair production:  $0-0.1 X_0$ ,  $0.1-0.2 X_0$ , and  $0.2-0.3 X_0$ . The division was made on the basis of the pulse-height spectra from the target-counter (its shape is similar to the curves of fig. 5). Figs. 8 and 9 show the energy spectra for the three regions of target thickness, without correction for ionisation and bremsstrahlung losses, and also with this correction. For convenience the curves have been normalized to the same area.

It should be noted that in our case the bremsstrahlung losses have not been considered completely, since the  $\gamma$ -counter aperture is only  $\pm 3.5^\circ$  and many  $\gamma$ -rays do not hit the counter. This is especially true

for large pair-production depths, for which the multiple scattering angles are large.

For comparison of the main characteristics of the present spectrometer with high-efficiency pair spectrometers of other laboratories we have compiled table 2.

TABLE 2

No. Laboratory	Year	Pair detection method	Resolution (%)	Target thickness (rad. length)
1. Dubna <sup>4)</sup>	1958	counters	6-9	0.007-0.03
2. Berkely <sup>7)</sup>	1964	counters	6-17	0.01-0.06
3. Liverpool <sup>8)</sup>	1967	spark chambers	3	0.015
4. Present work		spark chambers	1.5 2.3	0.014 0.1

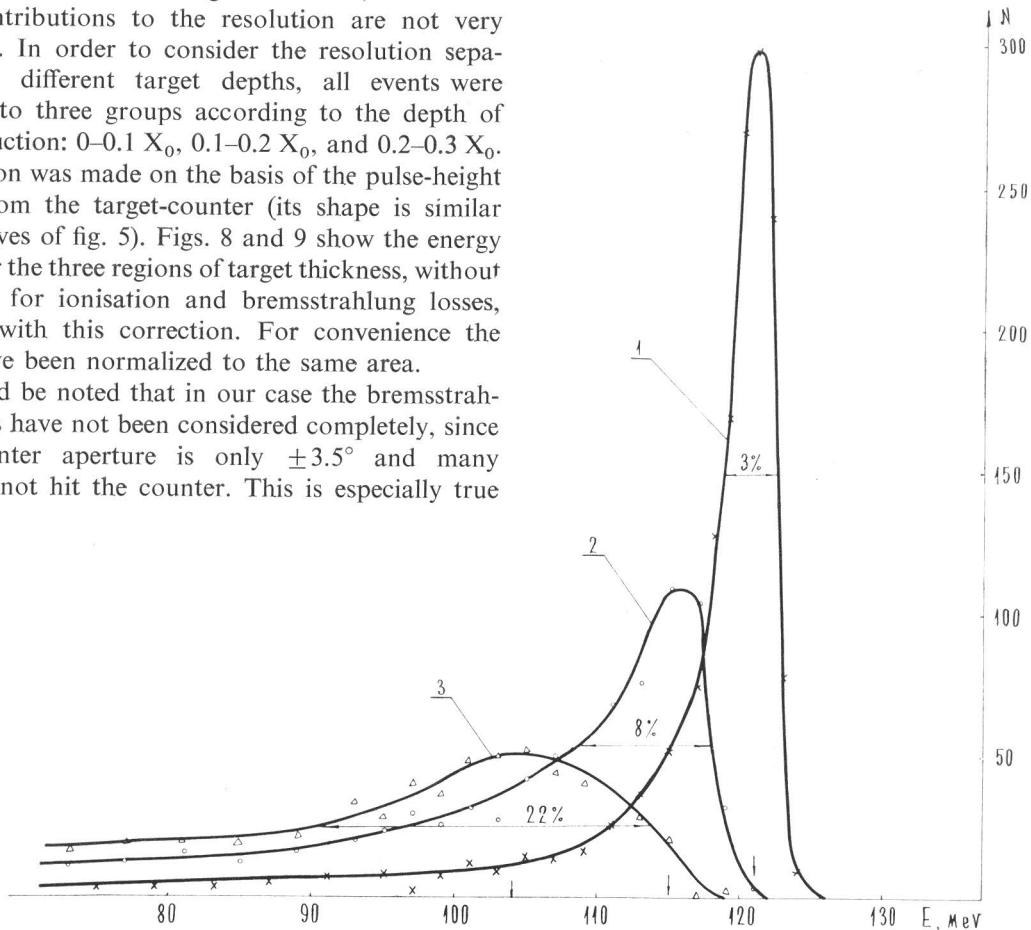


Fig. 8. Gamma-ray energy spectrum, without correction for ionisation and bremsstrahlung losses, for three regions of target thickness:  $0-0.1 X_0$ ,  $0.1-0.2 X_0$  (2);  $0.2-0.3 X_0$  (3). The curves are normalized to the same area.

The spectrometers 1 and 2 were designed for energies up to 600 MeV, and the resolution given is theoretical. Spectrometer 3 was designed for energies up to 20 MeV, and the resolution is experimental. For our spectrometer we have given the experimental resolution values, and the target thickness  $0.1 X_0$  is the effective thickness.

In conclusion we wish to thank the large group of coworkers who have taken part in preparation and calibration of the spectrometer and in processing of the results.

## References

- 1) B. S. Dzhelepov, Doklady AN SSSR **23** (1939) 25.
- 2) R. Walker and B. McDaniel, Phys. Rev. **74** (1948) 315.
- 3) W. Panofsky, R. Aamodt and J. Hadley, Phys. Rev. **81** (1951) 565.
- 4) Yu. D. Bayakov, M. S. Kozodaev, A. A. Markov, A. N. Sinaev and A. A. Tyapkin, PTE **6** (1958) 23 (Transl.: Instr. Exp. Techn.).
- 5) Yu. M. Ado, K. A. Belovintsev and S. N. Stolyarov, Atomn. Energ. **12** (1962) 193 (Transl. Soviet Atomic Energy).
- 6) B. S. Dolbilkin, V. A. Zapevalov, V. I. Korin and F. A. Nikolaev, JETP **44** (1963) 866 (Translation: Soviet Physics JETP).
- 7) G. D. Mead, K. J. Cence and D. L. Lind, Rev. Sci Instr. **35** (1964) 708.
- 8) J. R. Leslie and I. G. Main, Nucl. Instr. and Meth. **47** (1967) 345.

- 9) J. Fischer, Proc. Intern. Conf. *Electromagnetic interactions at low- and intermediate energies* (Dubna, Febr. 1967) **4** (1967) p. 179.
- 10) L. S. Korobeinikov, L. M. Kurdadze, A. P. Onuchin, S. G. Popov and G. M. Tumaikin, Yadern. Fiz. **6** (1967) 84 (Transl. Soviet J. Nucl. Phys.).

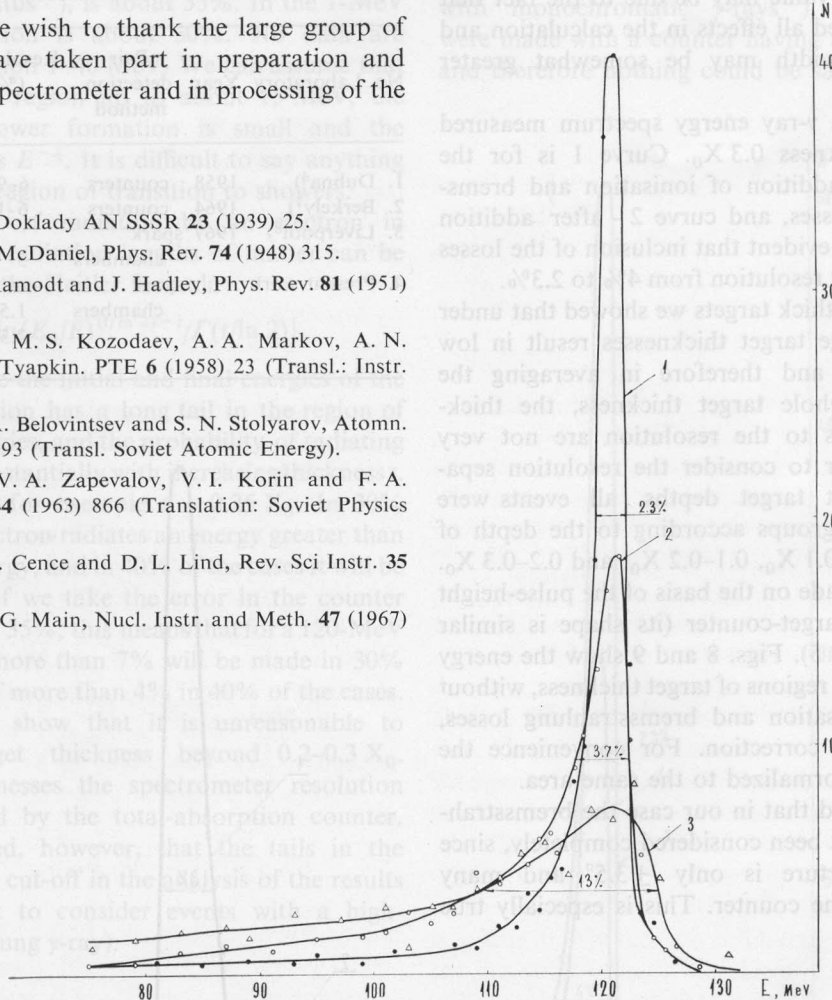


Fig. 9. Gamma-ray energy spectrum, after correction for ionisation and bremsstrahlung losses, for three regions of target thickness:  $0.01 X_0$  (1);  $0.1-0.2 X_0$  (2);  $0.2-0.3 X_0$  (3). The curves are normalized to the same area.